Resonant spin dipole induced by an in-plane potential gradient spin-orbit interaction

K. Y. Chen,[1] C. S. Chu,[1] and A. G. Mal'shukov[1,2,3]
[1]*Department of Electrophysics, National Chiao Tung University, Hsinchu 30010, Taiwan*
[2]*Institute of Spectroscopy, Russian Academy of Science, 142190 Troitsk, Moscow oblast, Russia*
[3]*National Center for Theoretical Sciences, Hsinchu 30043, Taiwan*
(Received 30 May 2007; published 11 October 2007)

Spin-orbit interaction (SOI) arising from in-plane potential gradient is invoked for the generation of spin accumulation in a driven electric field. The SOI and a local in-plane potential pattern together bring about resonant spin dependent scatterings to electrons in a nonequilibrium distribution. In the vicinity of a ring-shaped potential barrier pattern, a spin dipole distribution with a resonant dipole strength characteristic is obtained. As the chemical potential μ is increased across one such resonant energy, the dipole strength manifests both sign reversal and large amplitude enhancement. The scattering resonance, thus, provides an additional knob for the manipulation of the spin accumulation.

DOI: 10.1103/PhysRevB.76.153304 PACS number(s): 73.40.Lq, 72.25.Dc, 71.70.Ej

Spintronics exploits electron spin as the key physical entity for a new paradigm upon which novel device concepts and applications can be contrived.[1,2] The recent intensive studies on spin-Hall effect, where an external electric field leads to spin flow in the transverse direction, spin accumulation at lateral edges, and spin polarization in the bulk,[3–14] demonstrate great interest in nonmagnetic generation of spin transport and accumulation in semiconductors.

The spin-orbit coupling λ is much larger in semiconductors than in vacuum by a factor of, typically, 6 orders of magnitude. This factor is the ratio of the Dirac gap (m_0c^2 =0.5 MeV) in vacuum and an effective Dirac gap (E_g $\sim$1 eV) in semiconductor.[15,16] Various spin-orbit interactions (SOIs) have been considered. Of intrinsic nature are the Rashba[4,7,9–13] and Dresselhaus SOIs,[6,11] and of extrinsic nature is the impurity-induced SOI.[3,5,8,10,13] The Rashba SOI originates from a structure inversion asymmetry—the asymmetry in the confinement potential normal to a quantum well (QW). The Dresselhaus SOI originates from the inversion asymmetry in the crystal potential. The impurity-induced SOI is the atomiclike SOI albeit occurring in a semiconductor host. We point out that the SOI due to in-plane potential gradient has largely been neglected even though there have been studies on scattering by microstructures in SOI two-dimensional electron gas (2DEG).[17–21] An exception is a study on a smooth lateral potential.[17] It is then of interest to invoke the in-plane potential gradient SOI, to propose a relevant local in-plane potential pattern, and to study their resonant interplay. Very recently, strong in-plane gradient of the crystal potential in the surface layer of Bi/Ag(111) alloy is identified as the major physics behind a giant spin splitting.[22] Thus, the physics we explore here could also be of relevance to surface spintronics in metallic alloys.

Of our major concern here is the in-plane potential gradient SOI from a ring-shaped potential barrier (RSPB) in a symmetric QW, as shown in Fig. 1. The Rashba SOI is negligible in a symmetric QW, and the impurity-induced SOI effect turns out to be small. Expecting the physical picture to remain intact with the negligence of the Dresselhaus SOI, we leave the inclusion of it to future investigation. Driven by an electric field, electrons in a nonequilibrium distribution are scattered by the RSPB. The scattering is spin dependent and asymmetric with respect to the scattering angle. It leads to a simultaneous pileup of charge and spin dipoles, within the ballistic range of the ring, which orient oppositely and transversely to the electric field, respectively. The charge dipole is the Landauer residual resistivity dipole.[23,24] In a different system, a spin dipole has also been found near the vicinity of a non-SOI scatterer in a Rashba SOI host.[25,26] Our main result is that in-plane potential gradient SOI combined with transmission of a ring structure gives rise to a spin dipole of sufficiently large strength. As the Fermi energy is tuned across a resonant value, the spin dipole strength exhibits both large amplitude enhancement and sign reversal.

The RSPB $V(\rho)$ contributes to the SOI through a term of the form $-(\lambda/\hbar)\frac{1}{\rho}\frac{dV(\rho)}{d\rho}\mathbf{L}\cdot\boldsymbol{\sigma}$, where $\lambda \approx \frac{P^2}{3}\left[\frac{1}{E_g^2}-\frac{1}{(E_g+\Delta_0)^2}\right]$ =120 Å^2 for InAs,[15,16,27] $\mathbf{L}$ and $\boldsymbol{\sigma}$ are the orbital and the spin operator, and Δ_0 and P are, respectively, the energy of the split-off hole and the momentum matrix element between s and p orbitals. $\mathbf{L}\cdot\boldsymbol{\sigma}=L_z\sigma_z$ in a thin semiconductor film or a QW. Thus, for a plane wave $\varphi_{\mathbf{k}\sigma}=e^{i\mathbf{k}\cdot\mathbf{r}}\chi_\sigma$ incident in the x direction, where $\sigma_z\chi_\sigma=\sigma\chi_\sigma$ and $\sigma=\pm1$, the spin does not flip but the scattering is spin dependent. Cylindrical symmetry requires the total wave function in the form

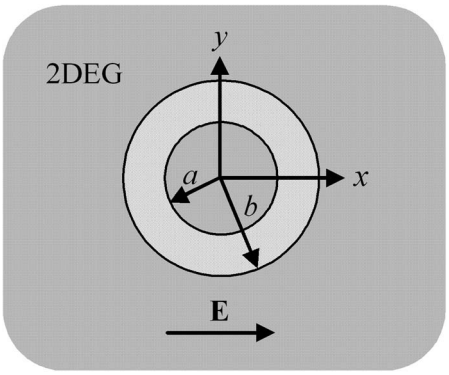

FIG. 1. System configuration: A ring-shaped potential pattern in a two-dimensional electron gas (2DEG), with radii a and b. An electric field $\mathbf{E}$ sets up a current in the 2DEG.

$$\Psi_{\mathbf{k}\sigma}(\boldsymbol{\rho}) = \sum_{l=-\infty}^{l=+\infty} i^l R_l^\sigma(\rho) e^{il(\phi_\rho - \phi_k)} \chi_\sigma, \tag{1}$$

where l, ϕ_ρ, and ϕ_k are the azimuthal angular momentum quantum number and angles of $\boldsymbol{\rho}$ and $\mathbf{k}$ with $\hat{x}$, respectively. $R_l^\sigma(\rho)$ satisfies the equation

$$\frac{1}{\rho}\frac{d}{d\rho}\rho\frac{d}{d\rho}R_l^\sigma + \left[k^2 - \frac{2m^*}{\hbar^2}\left(V - \frac{\lambda}{\rho}\frac{dV}{d\rho}l\sigma\right) - \frac{l^2}{\rho^2}\right]R_l^\sigma = 0, \tag{2}$$

with the particle energy $E=\hbar^2k^2/2m^*$. For a ring-shaped barrier, $V(\rho)=V_0[\theta(\rho-a)-\theta(\rho-b)]$, with a and b the inner and the outer radius, respectively, the radial function $R_l^\sigma(\rho)$ has the form

$$R_l^\sigma(\rho) = \begin{cases} C_{l\sigma}J_l(k\rho), & \rho < a \\ A_{l\sigma}[J_l(\kappa\rho) - B_{l\sigma}Y_l(\kappa\rho)], & a < \rho < b \\ e^{i\delta_l^\sigma}[\cos\,\delta_l^\sigma J_l(k\rho) - \sin\,\delta_l^\sigma Y_l(k\rho)], & b < \rho, \end{cases} \tag{3}$$

where $J_l(k\rho)$ and $Y_l(k\rho)$ are Bessel functions of the first and the second kind, respectively, $\kappa=\sqrt{k^2-2m^*V_0/\hbar^2}$ is the wave vector in the barrier region, and δ_l^σ is the phase shift, which we obtain to be

$$\delta_l^\sigma = \tan^{-1}\left[\frac{kbJ_l'(kb) - \gamma_{l2}^\sigma J_l(kb)}{kbY_l'(kb) - \gamma_{l2}^\sigma Y_l(kb)}\right]. \tag{4}$$

Here, $\gamma_{li}^\sigma = \left[\rho\frac{d\ln R_l^\sigma}{d\rho}\right]_{\rho=d_i-0^+} \mp \frac{2m^*\lambda l\sigma V_0}{\hbar^2}$, where $i=1$ (2) denotes $d_i=a$ (b) and upper (lower) sign, $B_{l\sigma} = \left[J_l'(\kappa a) - \frac{\gamma_{l1}^\sigma}{\kappa a}J_l(\kappa a)\right] / \left[Y_l'(\kappa a) - \frac{\gamma_{l1}^\sigma}{\kappa a}Y_l(\kappa a)\right]$, and $J_l'(x)=dJ_l(x)/dx$. Taking the limit $a=b$, one would get $\delta_l^\sigma=0$, as it should.

Resonant energies are obtained from the energy dependence of the phase shift, at which δ_l^σ deviates from its smooth general trend and exhibits abrupt change across a value of $\delta_l^\sigma=\pi/2$. More than one resonant characteristics can be found in δ_l^σ for a given l. These are associated with radial quantum number n. The excellent alignment of low lying resonant energies with the bound state energies of a cylindrical hard wall of radius a corroborates the role of quantum number n in the δ_l^σ resonances. S-wave ($l=0$) resonances in δ_l^σ, however, will not show up in the spin dipole resonance for the zero value of the SOI.

Driven by $\mathbf{E}=E_0\hat{x}$, the nonequilibrium electron distribution $g(\mathbf{k}) = -\frac{e\tau\hbar}{m^*}\mathbf{E}\cdot\mathbf{k}\,\delta(\varepsilon_\mathbf{k}-\mu)$, where $e>0$ and τ and μ are, respectively, the momentum relaxation time and the chemical potential. The spin density, with spin in units of $\hbar/2$, is given by

$$S_z(\boldsymbol{\rho}) = \frac{1}{4\pi^2}\int d\mathbf{k}\, g(\mathbf{k}) \sum_\sigma \sigma \Psi_{\mathbf{k}\sigma}^\dagger(\boldsymbol{\rho})\Psi_{\mathbf{k}\sigma}(\boldsymbol{\rho}), \tag{5}$$

which can be simplified to

$$S_z(\boldsymbol{\rho}) = n_E\,\mathrm{Re}\sum_\sigma \sigma \sum_{l=0}^{\infty} R_l^\sigma(\rho)R_{l+1}^{\sigma*}(\rho)\sin\,\phi_\rho \tag{6}$$

by the use of the relation $R_l^\sigma=(-1)^lR_{-l}^{-\sigma}$. The factor $n_E = \frac{eE_0\pi k}{\pi\hbar}$ depends linearly on E_0, and k is the Fermi wave vector corresponding to the Fermi energy μ. The angular dependence, $\sin\,\phi_\rho$, of the spin density $S_z(\boldsymbol{\rho})$ in Eq. (6) indicates a dipole distribution: aligned both in-plane and normal to $\mathbf{E}$. The spin density expression holds within a mean free path distance from the ring.

Presentation of our result is facilitated by a spin dipole strength p_s defined from the asymptotic behavior ($k_F\rho \gg 1$). Averaging out the Friedel oscillations, the asymptotic expression of S_z and its lowest correction term is given by

$$S_z = \frac{\sin\,\phi_\rho}{k^*\rho}\left[p_s + \frac{\wp_s}{k^*\rho}\right], \tag{7}$$

where

$$p_s = -\frac{n_E^* k\sigma_\perp}{4\pi}. \tag{8}$$

The constant factor n_E^* represents a typical value of n_E in Eq. (6), with Fermi wave vector k replaced by a typical value k^*. Casting into the form $n_E^* = \frac{m^*eE_0l_0^*}{\pi\hbar^2}$, with $l_0^*=\hbar k^*\tau/m^*$, its meaning is clearly shown to be the product of the two-dimensional density of states, $m^*/(\pi\hbar^2)$, and the work done $eE_0l_0^*$ by the electric field within l_0^*. Specific value of k^* depends on the system of our interest, and will be chosen in the following numerical example. The factor $k\sigma_\perp$ is essentially a transverse moment of the spin dependent part of the differential cross section $D_\sigma(\phi)$, given by $\sigma_\perp = \int_0^{2\pi} d\phi \sin\,\phi \Sigma_{\sigma'}\sigma' D_{\sigma'}(\phi)$, where $D_\eta(\phi) = \frac{1}{2\pi k}\left|\Sigma_{l=0}^\infty (e^{2i\delta_l^\eta} - 1)e^{il\phi}\right|^2$. In terms of the phase shifts,

$$\sigma_\perp = \frac{2}{k}\sum_\sigma \sigma \sum_{l=0}^{\infty} \sin[2(\delta_l^\sigma - \delta_{l+1}^\sigma)], \tag{9}$$

$\wp_s = \frac{1}{4\pi}n_E^*k^*\sigma_\perp'$ and $\sigma_\perp' = \frac{1}{k}\Sigma_\sigma\sigma\Sigma_{l=0}^\infty(2l+1)\cos[2(\delta_l^\sigma - \delta_{l+1}^\sigma)]$. Our key results are in Eqs. (6)–(9).

In Fig. 2, we present the μ dependence of $k\sigma_\perp$. Parameter units typical for InAs are electron density $n_e^*=7.4\times10^{11}$ cm^{-2}, energy unit $E^*=n_e^*\pi\hbar^2/m^*=77.1$ meV, $m^*=0.023m_e$, $k^*=2.16\times10^8$ m^{-1}, and length unit $L^*=1/k^*=46.3$ Å. In these units, the ring-shaped potential has radii $a=14$ and $b=20.5$, barrier potential $V_0=0.75$, mean free path $l_0^*=238$, and $E_0=0.1$ kV/cm. The spin dipole strength p_s is fully characterized by $k\sigma_\perp$ except for a factor $n_E^*/4\pi=8.4\times10^9$ cm^{-2}. As shown in Fig. 2(a), $k\sigma_\perp$ contains many resonant structures: each resonance is represented by a pair of peak and dip spikes. The resonant enhancement is large: away from resonances, $|k\sigma_\perp|\approx10^{-1}$, but at resonance, its maximum magnitude can reach up to 7 such that the enhancement factor reaches 70. The resonant profile invites grouping into different series, each associated with a radial quantum number n. The first ($n=1$) series starts from $\mu=0.064$, consisting of the largest resonant amplitudes, and with l starting from $l=1$ and onward until over 16. The n

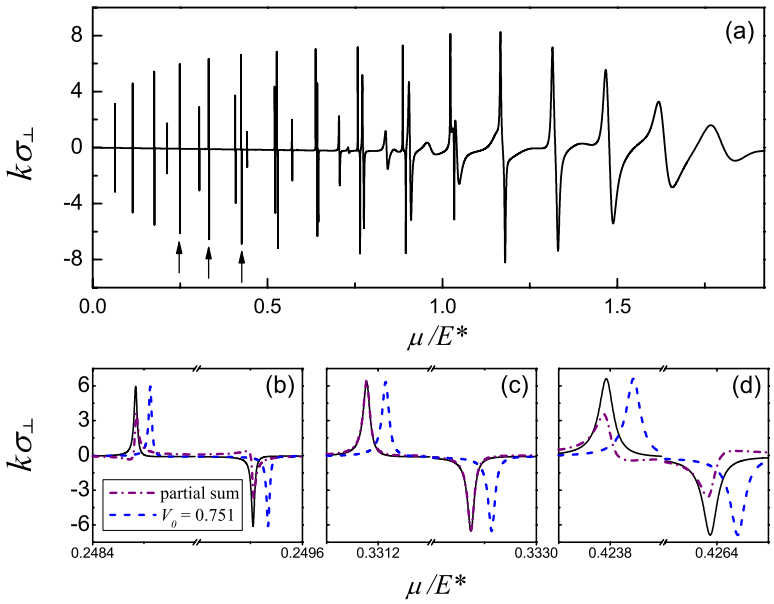

FIG. 2. (Color online) (a) $k\sigma_\perp$ versus the Fermi energy μ, with energy unit $E^*=77.1$ meV. The radii of the RSPB are $a=14$ and $b=20.5$, respectively, and $V_0=0.75$. (b)–(d) Blowups of the $n=1$, $l=4,5,6$ resonances, respectively. The dotted-dashed (purple) curves represent partial summations of $k\sigma_\perp$, including only terms that involve $\delta^\sigma_{l=5}$. The dashed (blue) curves are the full summation for the case of $V_0=0.751$. The smallest abscissa division in (b)–(d) is 0.0001.

$=2$ and $n=3$ series start from $\mu=0.213$ and $\mu=0.44$, respectively. The low lying resonant energies ($\mu \ll 0.75$) align very well with the bound state energies in a cylindrical hard wall of radius a. Higher resonant energies are slightly redshifted relative to the bound state energies, while the resonant widths are widened.

Further confirmation that each peak-dip resonant pair in $k\sigma_\perp$ is due to a single resonance event is obtained by close inspection of the resonant pairs: the ($n=1$, $l=4,5,6$) resonances in Figs. 2(b) and 2(c), respectively. The solid curves are full summations of $k\sigma_\perp$ according to Eq. (9); the dotted-dashed curves are partial summations of $k\sigma_\perp$, including only terms that involve $\delta^\sigma_{l=5}$; and the dashed curves are the full summation of $k\sigma_\perp$, but for $V_0=0.751$. The dotted-dashed curve matches very well with the (1,5) structure, but reproduces only qualitative features for the (1,4) and (1,6) structures. Thus, the resonant pair at $l=5$ is directly associated with the resonant behavior of the phase shift $\delta^\sigma_{l=5}$. That the same partial summation also reproduces qualitative resonance features for $l=14$ and $l=16$ is because the partial summation has included some but not all terms involving $\delta^\sigma_{l=4}$ and $\delta^\sigma_{l=6}$. The effect of increasing V_0 is shown to cause blue-shifted and sharper resonant structures, which, again, corroborate our scattering resonance picture.

The summation expression of $k\sigma_\perp$ in Eq. (9) is also useful in understanding the origin of the peak-dip pair at each resonance. Setting λ to zero, the summation $\Sigma_{l=0}^{\infty} \sin[2(\delta_l^\sigma - \delta_{l+1}^\sigma)]$ becomes spin independent, with peaks at the resonant energy E^0_{nl}. Recovering λ, the peak energy is shifted to E^σ_{nl}, with the direction of energy shift opposite for opposite spin. It is the difference between these two shifted peaks that gives rise to the peak-dip pairs in $k\sigma_\perp$. Interesting competition feature can also be observed in Fig. 2(a). The peak-dip pairs in an n series trace out an envelope, the amplitude of which increases in low l and decreases at high l. This demonstrates the competition between the trend of stronger SOI for larger l and the trend of weakening of the resonance due to wider resonance width at higher energy.

In Fig. 3, we present the radial variation of the spin density $S_z(\rho)$. Energies at 0.3312 [Fig. 3(a)] and 0.3328 [Fig. 3(b)], are the peak and dip energies, respectively, of the $l=5$ resonance in Fig. 2. The dashed curves denote the first term in Eq. (7), and the dotted-dashed curves are the adjusted asymptotic behavior, including the φ_s term. Apart from the Friedel oscillations, the dotted-dashed curves trace the asymptotic spin distribution remarkably. Figures 3(a) and 3(b) show that the sign of the spin density can be reversed by a small change in $\Delta\mu=0.0016E^*$, or 0.12 meV. The spin

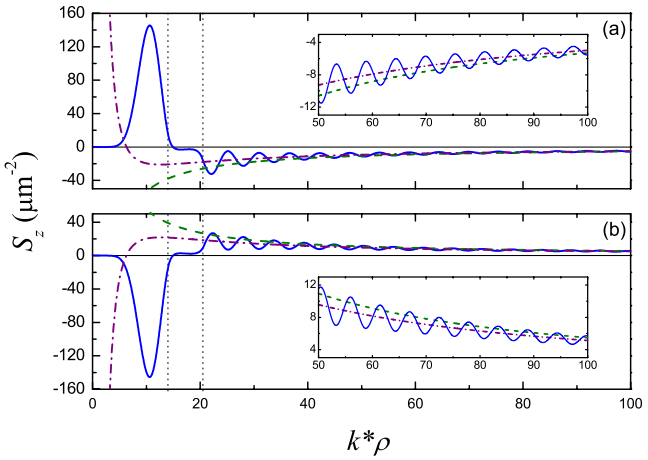

FIG. 3. (Color online) Radial dependence of $S_z(\rho)$ for $\phi=\pi/2$ and for $\mu/E^*=0.3312$ (a) and 0.3328 (b), corresponding, respectively, to the peak and the dip of the $l=5$ resonance in $k\sigma_\perp$ in Fig. 2. The dashed (green) and dotted-dashed (purple) curves are, respectively, the asymptotic behavior characterized by p_s and the adjusted asymptotic behavior when φ_s is also included. The vertical dotted lines denote the ring region. At $k^*\rho=50$, $S_z=-9.276$ μm^2 (a) and 9.568 μm^{-2} (b), respectively.

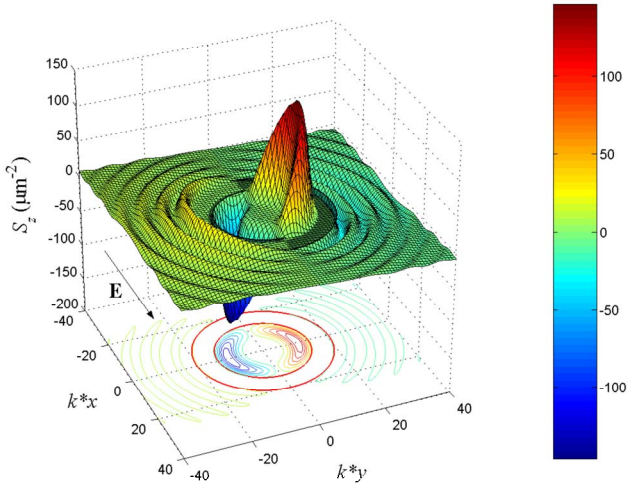

FIG. 4. (Color online) Spatial distribution of $S_z(\boldsymbol{\rho})$. Fermi energy $\mu/E^*=0.3312$ for the Fig. 3(a) case, and **E** is along $\hat{x}$. The ring region is denoted both by the gray circular bar and by the concentric circles on the projected $x=y$ plane.

density at $k^*\rho=50$, $\rho=0.23$ μm, is (a) -9.276 μm^{-2} and (b) 9.568 μm^{-2} or, in terms of the electron density $n=2.45\times10^{11}$ cm^{-2}, the spin density is (a) 0.379% and (b) 0.39%, respectively, of n, which is certainly large enough for observation.[28] The spin density at $k^*\rho=100$ is one-half of the above results. Finally, in Fig. 4, we present both the radial and the angular dependence of the spin dipole for the case of $\mu=0.3312$.

The proposed RSPB pattern is expected to be within reach by recent development in integrating focused ion beam and molecular beam epitaxy,[29] where patterned δ-doped layers are fabricated. The steplike potential profile model offers a clear physical picture, and the results remain qualitatively intact if the potential profile is replaced by a smooth profile.[30]

In conclusion, we have shown that the in-plane potential gradient SOI and scattering resonance together can give rise to significant spin polarization. In our case here, it is in the form of a spin dipole, and the enhancement factor from resonance is large. Finally, the resonance provides us an important feature: an electrical way of switching the sign of the accumulated spin density by a simple control of the electron density.

The work was supported by the National Science Council of ROC under Grants No. NSC95-2112-M-009-004 and No. NSC93-2119-M-007-002 (NCTS), the RFBR Grant No. 060216699, and the MOE-ATU grant. The authors are grateful to the Center for Advanced Study in Oslo for hospitality. One of the authors (C.S.C.) acknowledges useful discussion with S. Q. Shen and the hospitality of the University of Hong Kong.

[1] *Semiconductor Spintronics and Quantum Computation*, edited by D. D. Awschalom, N. Samarth, and D. Loss (Springer-Verlag, Berlin, 2002).
[2] I. Zutic, J. Fabian, and S. Das Sarma, Rev. Mod. Phys. **76**, 323 (2004).
[3] M. I. D'yakonov and V. I. Perel, JETP Lett. **13**, 467 (1971).
[4] V. M. Edelstein, Solid State Commun. **73**, 233 (1990).
[5] J. E. Hirsch, Phys. Rev. Lett. **83**, 1834 (1999).
[6] S. Murakami, N. Nagaosa, and S. C. Zhang, Science **301**, 1348 (2003).
[7] J. Sinova, D. Culcer, Q. Niu, N. A. Sinitsyn, T. Jungwirth, and A. H. MacDonald, Phys. Rev. Lett. **92**, 126603 (2004).
[8] Y. K. Kato, R. C. Myers, A. C. Gossard, and D. D. Awschalom, Science **306**, 1910 (2004).
[9] J. Wunderlich, B. Kaestner, J. Sinova, and T. Jungwirth, Phys. Rev. Lett. **94**, 047204 (2005).
[10] H. A. Engel, B. I. Halperin, and E. I. Rashba, Phys. Rev. Lett. **95**, 166605 (2005).
[11] A. G. Mal'shukov, L. Y. Wang, C. S. Chu, and K. A. Chao, Phys. Rev. Lett. **95**, 146601 (2005).
[12] J. Sinova, S. Murakami, S. Q. Shen, and M. S. Choi, Solid State Commun. **138**, 214 (2006).
[13] W. K. Tse and S. DasSarma, Phys. Rev. B **74**, 245309 (2006).
[14] S. Q. Shen, Phys. Rev. Lett. **95**, 187203 (2005).
[15] E. I. Rashba, Physica E (Amsterdam) **34**, 31 (2006).
[16] R. Winkler, *Spin-orbit Coupling Effects in Two-dimensional Electron and Hole System* (Springer-Verlag, Berlin, 2003).
[17] A. O. Govorov, A. V. Kalameitsev, and J. P. Dulka, Phys. Rev. B **70**, 245310 (2004).
[18] H. Chen, J. J. Heremans, J. A. Peters, A. O. Govorov, N. Goel, S. J. Chung, and M. B. Santos, Appl. Phys. Lett. **86**, 032113 (2005).
[19] J. D. Walls, J. Huang, R. M. Westervelt, and E. J. Heller, Phys. Rev. B **73**, 035325 (2006).
[20] J. Y. Yeh, M. C. Chang, and C. Y. Mou, Phys. Rev. B **73**, 035313 (2006).
[21] A. Pályi, C. Péterfalvi, and J. Cserti, Phys. Rev. B **74**, 073305 (2006).
[22] C. R. Ast, J. Henk, A. Ernst, L. Moreschini, M. C. Falub, D. Pacilé, P. Bruno, K. Kern, and M. Grioni, Phys. Rev. Lett. **98**, 186807 (2007).
[23] R. Landauer, IBM J. Res. Dev. **1**, 223 (1957); Philos. Mag. **21**, 863 (1970).
[24] R. S. Sorbello and C. S. Chu, IBM J. Res. Dev. **32**, 58 (1988); C. S. Chu and R. S. Sorbello, Phys. Rev. B **38**, 7260 (1988).
[25] A. G. Mal'shukov and C. S. Chu, Phys. Rev. Lett. **97**, 076601 (2006).
[26] A. G. Mal'shukov, L. Y. Wang, and C. S. Chu, Phys. Rev. B **75**, 085315 (2007).
[27] P. Noziéres and C. Lewiner, J. Phys. (Paris) **34**, 901 (1973).
[28] V. Sih, W. H. Lau, R. C. Myers, V. R. Horowitz, A. C. Gossard, and D. D. Awschalom, Phys. Rev. Lett. **97**, 096605 (2006).
[29] T. Hada, T. Goto, J. Yanagisawa, F. Wakaya, Y. Yuba, and K. Gamo, J. Vac. Sci. Technol. B **18**, 3158 (2000).
[30] K. Y. Chen, C. S. Chu, and A. G. Mal'shukov (unpublished).